

Phase transition in tumor growth VIII: The spatiotemporal avascular evolution

P. J. Betancourt-Padron^a, K. García-Medina^b, R. Mansilla^{c,*}, and J. M. Nieto-Villar^{a,*}

^a*Department of Chemical-Physics, A. Alzola Group of Thermodynamics of Complex Systems of M.V. Lomonosov Chair, Faculty of Chemistry, University of Havana, Cuba.
e-mail: nieto@fq.uh.cu*

^b*Department of Applied Physics, Physics Faculty, University of Havana, Cuba.*

^c*Centro de Investigaciones Interdisciplinarias en Ciencias y Humanidades, UNAM, México.
e-mail: mansy@unam.mx*

Received 1 July 2020; accepted 13 August 2020

A 2D cellular automata model, which allows a better understanding of the morphogenesis of the avascular tumor pattern formation, is presented. Using thermodynamics formalism of irreversible processes and results of complex systems theory, we propose features that establish, in a quantitative way, the degree of aggressiveness and the malignancy of tumor patterns, such as a fractal dimension and the entropy production rate.

Keywords: Biological phase transition; cellular automata; avascular tumor growth; entropy production rate; fractal dimension.

PACS: 87.15.Zg; 02.70.-c; 87.19.xj; 05.70.-a; 05.70.Ln; 05.45.Df; 61.43.-j

DOI: <https://doi.org/10.31349/RevMexFis.66.856>

1. Introduction

According to the WHO [1], cancer is the second leading cause of death worldwide, and it is estimated that the number of new cases will increase in the coming years. There is enough evidence [2,3] regarding the complexity of cancer. We mean that cancer is seen as a self-organizing non-linear dynamic system, far from thermodynamic equilibrium [4,5,6], exhibits a fractal structure that allows it to evade the action of the immune system and host cells [7-12]. Shows growth dynamics in the metastatic stage, deterministic chaos type, which confers high robustness, poor long-term prognosis, adaptability, and learning capacity [13-16].

As we have shown in previous works [16], cancer can be seen as a complex network made up of cells that have lost their specialization and growth control, and that emerges through what we can call “biological phase transition” [17-19].

Cancer evolution and emergence are known to occur through three distinct stages (avascular, vascular, and metastatic) [20]; researchers often concentrate their efforts on answering specific questions on each of these stages. In the avascular phase, the tumor grows to a state known as a dormant state [21], with microscopic characteristics, this process, occurs through a “second-order” phase transition [19] through either logistic or Gompertz dynamic equations equivalently [19], which corresponds to the fact that such growth occurs silently.

The avascular phase, dormant state [22], is a stable stationary state, taking on a spheroid shape of a few millimeters in diameter, whose histological examination shows three different concentric annular layers [23,24]. Proliferating cells [7] are found in the thinner outer layer with a rough edge,

fractal [7]. In the contiguous layer, typically three times thicker than the proliferation layer, inactive cells, quiescent cells, exhibit little or no proliferation. The innermost nucleus consists of necrotic remains [25]. The tumor can remain in this latent state for months or even years, reaching a size between 1-2 mm in diameter and cannot be detected on a macroscopic scale [26]; therefore, its detection is usually limited.

This work aims to generalize the previously proposed model of avascular tumor growth [19] with the inclusion of spatiotemporal behavior. The manuscript is organized as follows: In Sec. 2, a two-dimensional (2D) cellular automata model is presented for the spatiotemporal study of avascular tumor growth. Section 3 describes the experimental part: the spatiotemporal avascular growth, including the dynamical behavior, the fractal dimension, and the entropy production rate of the tumor patterns. Finally, some concluding remarks are presented.

2. A Two-Dimensional (2D) Cellular Automata Model for the Spatiotemporal of Avascular Tumor Growth

Mathematical models [27] represent a language for formalizing the knowledge on living systems obtained in theoretical biology [28,29,30]. Basic models of tumor growth [31,32] make the description of the principal regularities possible and are a useful guideline for cancer therapy, drug development, and clinical decision-making.

These models can be classified into two general groups: deterministic based on ordinary or partial differential equations (ODEs, PDEs) [33] and stochastic models [34-37]. On the other hand, to describe a spatial pattern formation

has been used indistinctly, PDEs [38], agent-based models (ABM) [39,40], particularly, cellular automata (CA) [41-43], hybrid cellular automaton [44], and multi-scale models [45].

CAs have been widely used given their ability to generate a broad spectrum of complex patterns from relatively simple rules which capture many behavioral characteristics and the complexity of real self-organizing systems far from thermodynamic equilibrium [39].

The advantage of CA models is that they can directly incorporate the rules that define the processes of mitosis and apoptosis, as pointed out by Basanta et al. [46] based on the presence of cancer cell hallmarks [47].

The proposed CA cellular automaton is a reinterpretation of the model of Pourhasanzade *et al.* [48], a two-dimensional (2D) stochastic agent-based model for the spatiotemporal study of avascular tumor growth. For the development of the CA model and spatial patterns, the Python 3 programming language was used [49].

The main differences with the model of Pourhasanzade *et al.* [48] are:

1. Only one type of proliferative cell (PT) with its respective probability of proliferation was considered, and it was the one that considers the microenvironment since this expression encompasses both expressions and represents a more comprehensive concept of tumor growth.
2. The immune system was not explicitly taken into account.

The proposed model is made up of a two-dimensional square lattice (2D, $n \times n$ cells); each cell in the lattice is defined by position coordinates (i, j) , where $0 < i, j \leq n$ cells. These agents can take 4 possible modes: **0** - normal cells (N); **1** - proliferative cells (PT); **2** - non-proliferative cells (NT); **3** - necrotic cells (Ne). Besides the empty spaces in the lattice are shown as agents in mode **0**.

The model includes a set of update rules at the cellular level of the biological system consisting of two sets of transition rules for agents. Thus, it considers proliferative cell mitosis (PT), competition between cell populations, and interaction between normal and tumor cells.

The transition rules for this model are probabilistic, and a Moore neighborhood [50] limits the interaction of each lattice site with its neighborhood. On the other hand, the nutrients are supposed to be evenly distributed in the lattice, where its deficiency can be considered due to the lack of free space within a certain distance from a cell. Therefore, a PT cell can only be divided with some probability into two daughter cells as long as there is a space in its vicinity, placing a daughter cell. In contrast, the other daughter cell will replace the position from which it originated.

Each mode 1 agent (PT cell) can proliferate with a probability as a function of time and space, such that

$$P = P_0 \times n_0 \times \left(1 - \frac{r}{R_{\max}}\right) \quad (1)$$

where P_0 is a base probability of proliferation, which in the original work by Pourhasanzade *et al.* [48] it is assigned an arbitrary value, in our case, according to the temporal model previously developed by us [19] we associate by ansatz to the quotient of the mitosis(ψ) /apoptosis(η) constants, $P_0(\psi/\eta)$, whose quotient characterizes a given tumor [51]. Consequently, the probability P of proliferative cells (PT) is associated with the rates of mitosis (V_m) and apoptosis (V_a), respectively.

The n_0 reflects the number of healthy cells (N) in each site's vicinity, associated with the morphological characteristics of the host tissue. The r is the position of each cell with respect to the center of the tumor and R_{\max} is a constant value that is prefixed and denotes the maximum diameter between 1-2 mm that the tumor can reach [52] since it is known that they grow in the avascular stage until they reach a latent state. Appendix A shows a flowchart showing the sets of rules for the agent-based model proposed.

In this way, it is ensured that the CA model results are adjusted through either logistic or Gompertz dynamic equations equivalently [19] and that it follows a dynamic where for radius greater than R_{\max} the probability of proliferation is zero, thus showing the effect of the mechanic pressure exerted by the host on tumor growth [24].

In each time iteration, if the agent mode is **1**, it is checked if the agent has opportunities to proliferate. For this, there must be at least one agent with mode **0** in its vicinity. If so, the corresponding PT cell will choose one of those possible positions at random and divide with a probability P . Of the two new cells created, one takes the position of the cell in mode **0**, and the other remains in the position of the PT cell.

In case the PT cell cannot proliferate, either because it cannot find a healthy neighbor in its vicinity or because it cannot proliferate with a probability P , it will remain as a PT cell for a certain time. Therefore, each PT cell has an age counter that is incremented at each time step and is reset if the cell undergoes mitosis. After reaching a certain time (age threshold), the PT cell can change to the NT cell, changing the mode from **1** to **2** when it is at a greater distance than δ_P , the one associated with a certain distance from the edge of the tumor.

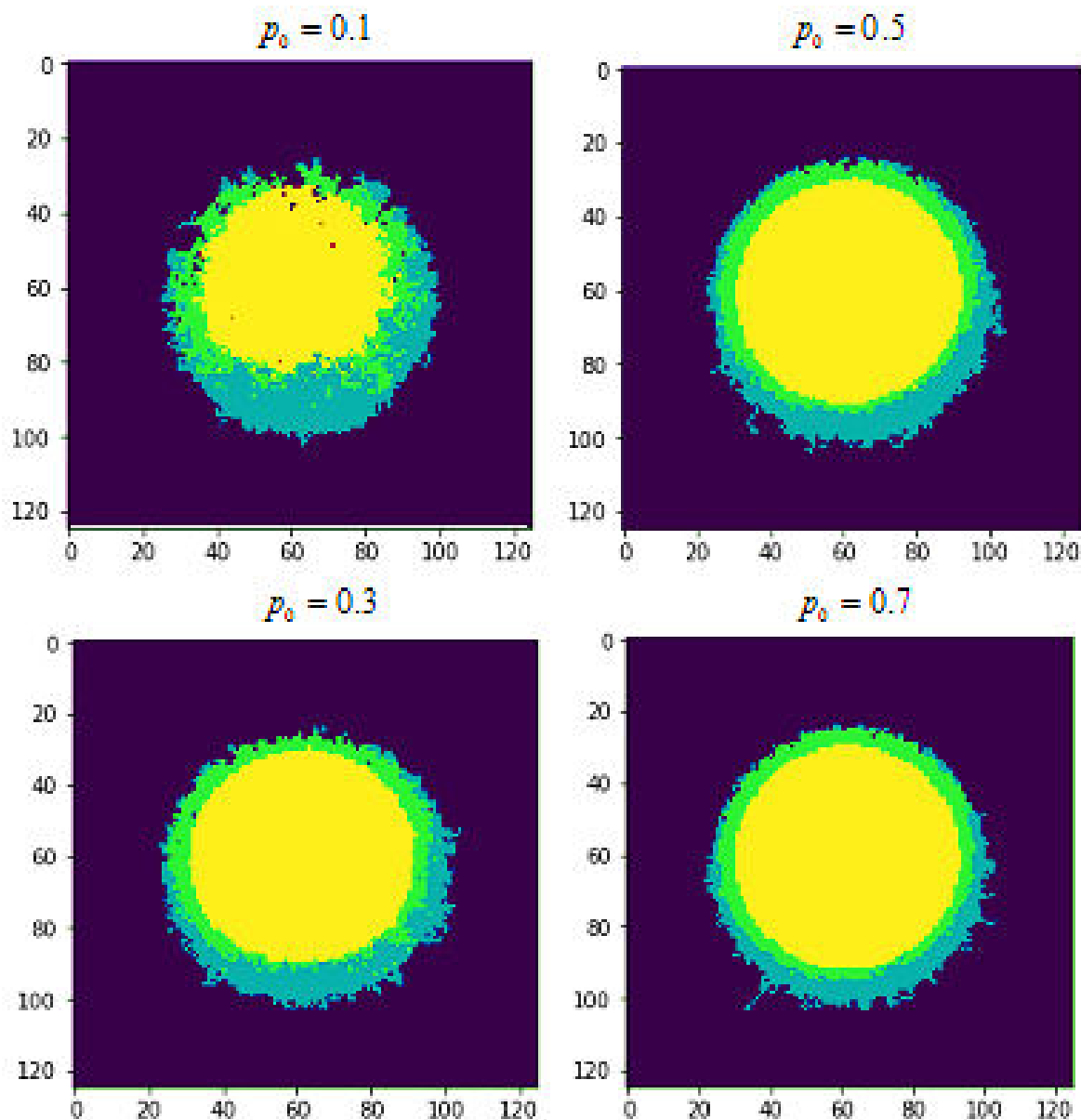
NT cells that are in mode **2** can change to Ne cells (necrotic cells, mode **3**) if they are at a greater distance than $\delta_P + \delta_n$ from the edge of the tumor due to the absence of nutrients. These Ne cells are found in the center of the tumor as a mass of dead cells and do not change their mode under any circumstances.

The radius of the necrotic region (R_n) and the thickness of the region of PT (δ_P) and NT cells (δ_n) are obtained by the following equations [40]:

$$\begin{aligned} R_n &= R_t - (\delta_P + \delta_n), \\ \delta_P &= bR_t^{2/3}; \quad \delta_n = aR_t^{2/3}, \end{aligned} \quad (2)$$

TABLE I. Parameters used in the model.

Parameters	Brief explanation	value
$P_0 \square \frac{\psi}{\eta}$	Baseline probability of proliferation of PT cells, associated with to the quotient of mitosis(ψ) / apoptosis(η) constants, see Eq. (1).	0.1; 0.3; 0.5; 0.7
R_{\max}	Maximum tumor extent, controlled by pressure of surrounding tissue, see Eq. (1).	37.5
a	Base necrotic thickness, controlled by the need for nutrients, see Eq. (2).	0.42
b	Proliferative base thickness, controlled by the need for nutrients, see Eq. (2).	0.11

FIGURE 1. Patterns formed during avascular growth obtained for different values of p_0 (0.1; 0.3; 0.5; 0.7) after 200 iteration steps have reached the dormant state: healthy tissue (N, purple), proliferative cells (PT, blue), non-proliferative cells (NT, green), necrotic (Ne, yellow).

where a and b are constant parameters that reflect the need for nutrients in tumor growth, and R_t is the average radius of the tumor. Table I shows the values of the parameters used in the CA model. In all cases, the parameters used are dimensionless.

3. Experimental Part: the Spatiotemporal Avascular Tumor Growth

Figure 1 shows the patterns that are obtained for different values P_0 after 200 iteration steps, when saturation is achieved, that is, the dormant state. In purple, it represents healthy tissue (N), blue is proliferative cells (PT), green is non-proliferative cells (NT), and yellow is necrotic (Ne).

For each fractal pattern (see Fig. 1), the fractal dimension d_f was determined using the box-counting method [53,54]. Each image was processed with the ImageJ 1.40 g software by Wayne Rasband, National Institute of Health, USA (<http://rsb.info.nih.gov/ij>).

As shown in previous work [36], the fractal dimension d_f can be given as a function of the quotient between mitosis (V_m) and apoptosis (V_a) rates [36,55], different values of d_f representing the “degree of malignancy” [56] which quantifies the capacity of the tumor to invade and infiltrate the healthy tissue, as

$$d_f = \frac{5 - \frac{V_m}{V_a}}{\frac{V_m}{V_a} + 1}. \tag{3}$$

From the Eq. (3) the quotient of mitosis/apoptosis rates (V_m/V_a) was determined (see Table II), which increases as the value of growths P_0 , which physically implies an increase in the degree of malignancy of the patterns formed. Notably, the fractal dimension values for the different patterns are in the range of values reported by Brú [7] for different tumor cell lines (see Fig. 1, Table II).

Figure 2 shows how the cell population varies with time, for different values P_0 after 200 iteration steps, so that saturation is achieved, that is, the dormant state (see Appendix B).

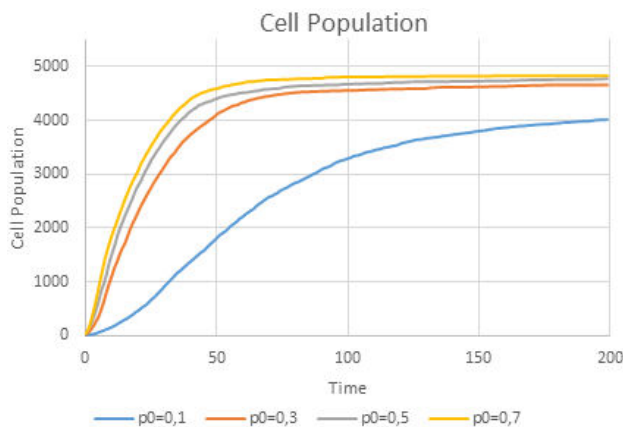


FIGURE 2. Temporal variation of the cell population (PT) for different values of P_0 (0.1; 0.3; 0.5; 0.7) after 200 iteration steps.

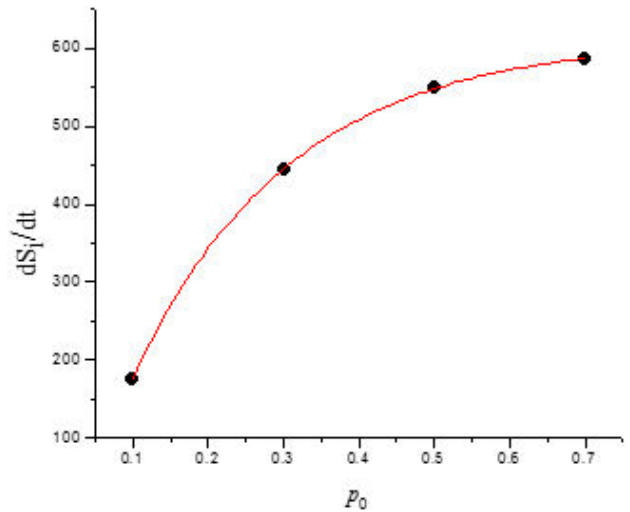


FIGURE 3. The entropy production rate \dot{S}_i for different values of p_0 .

TABLE II. Fractal dimension values d_f and quotient of mitosis/apoptosis rates (V_m/V_a) for each of the patterns (see Fig. 1) for different values of P_0 .

P_0	0.1	0.3	0.5	0.7
d_f	1.1869	1.1763	1.1324	1.1207
V_m/V_a	1.7436	1.7570	1.8137	1.8293

As observed, a sigma-shaped curve the avascular growth of the tumor, follows a growth dynamic, through either logistic or Gompertz dynamic equations equivalently [11,19]. As we pointed out in Sec. 2, the probability p of proliferative cells (PT) is associated with the rates of mitosis (V_m) and apoptosis (V_a), respectively. This shows how, for different types of tumors, characterized by their P_0 value, the tumor exhibit varying degrees of aggressiveness [19]. We previously reported [36] the same behavior that in this work is obtained for different types of tumor cell lines.

Previously we have shown [51] that the entropy production rate \dot{S}_i was determined for avascular tumor growth as a physical function of cancer robustness, such as

$$\dot{S}_i = R(V_m - V_a) \ln \left(\frac{5 - d_f}{1 + d_f} \right). \tag{4}$$

The Eq. (4) shows two major properties associated with the avascular tumor growth: The first is its growth rate, which is associated with its invasive capacity, mitosis (V_m), and apoptosis (V_a) rates, related with the degree of aggressiveness. The second is its complexity, a morphology characteristic, such as the fractal dimension of the tumor interface, associated with malignancy, which quantifies the tumor capacity to invade and infiltrate the healthy tissue [56]. Figure 3 shows the entropy production rate \dot{S}_i for different values of p_0 .

As can be seen, the entropy production rate \dot{S}_i shows how the robustness of the tumor increases as its invasive capacity

increases, degree of aggressiveness, and in turn, its malignancy.

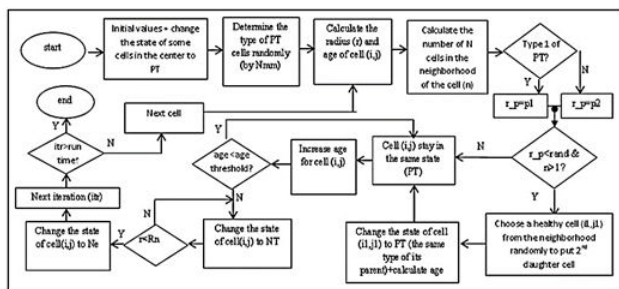
4. Conclusions and Remarks

In summary, in this paper, we have found that the proposed two-dimensional (2D) cellular automata model generalized the spatiotemporal behavior of avascular tumor growth, and that allows a better understanding of the morphogenesis of the tumor pattern formation.

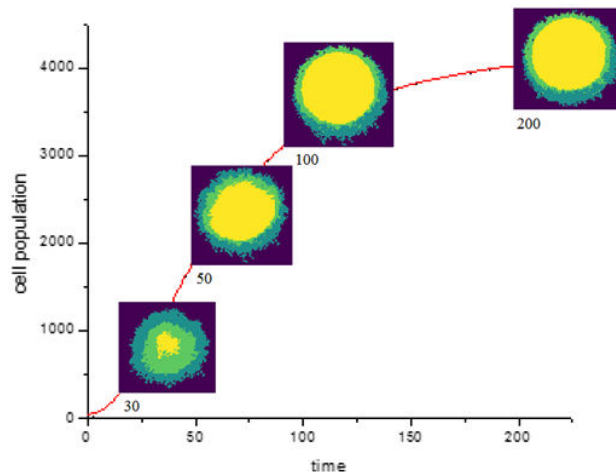
Using thermodynamics formalism of irreversible processes and complex systems theory, we propose and quantify markers able to establish, in a quantitative way, the degree of aggressiveness and the malignancy of tumor patterns, such as:

1. The tumor complexity, such as a fractal dimension, proves to be useful for describing the pathological architecture of tumors and for yielding insights into the mechanisms of tumor growth.
2. The entropy production rate is a physical hallmark of cancer robustness that allows us the possibility of prognosis of tumor proliferation and invasion capacities, key factors to improve cancer therapy.

The current theoretical framework will hopefully provide a better understanding of cancer growth and contribute to cancer treatment improvements.



APPENDIX A. Flowchart showing the sets of rules for agent-based model proposed.



APPENDIX B. Figure showing different time stages (30,50,100,200) of the spatial system for $p_0 = 0.3$.

Acknowledgments

Prof. Dr. A. Alzola and Prof. Dr. Germinal Cocho in memoriam. JMNv thanked the CEIICH of the UNAM Mexico for the warm hospitality and the financial support by PREIDGAPA-2019. RM appreciates the warm reception received at CEPHCIS of the National Autonomous University of Mexico, where part of this work was carried out. Finally, we thank the anonymous reviewers for their helpful comments and interesting suggestions.

1. <https://www.who.int/health-topics/cancer>
2. M. M. Gottesman, O. Lavi, M. D. Hall, and J. P. Gillet, Toward a better understanding of the complexity of cancer drug resistance. *Annual review of pharmacology and toxicology*, **56** (2016) 85. <https://doi.org/10.1146/annurev-pharmtox-010715-103111>
3. M. Bizzarri, et al. . Fractal analysis in a systems biology approach to cancer. *In Seminars in cancer biology* **21** (2011) 175. <https://doi.org/10.1016/j.semcancer.2011.04.002>

4. T. S. Deisboeck et al., Pattern of self-organization in tumour systems: complex growth dynamics in a novel brain tumour spheroid model, *Cell Prolif*, **34** (2001) 115. <https://doi.org/10.1046/j.1365-2184.2001.00202.x>
5. R. Rockmore, *Cancer complex nature*. Santa Fe Institute Bulletin **20** (2005) 18.
6. E. Izquierdo-Kulich and J. M. Nieto-Villar, *Morphogenesis and Complexity of the Tumor Patterns*, R.G. Rubio et al. (eds.), Without Bounds: A Scientific Canvas of Nonlinearity and Complex Dynamics. Understanding Complex Systems.

- Springer-Verlag Berlin Heidelberg (2013).
7. A. Brú, *et al.*, The universal dynamics of tumor growth, *Biophysical journal*, **85** (2003) 2948. [https://doi.org/10.1016/S0006-3495\(03\)74715-8](https://doi.org/10.1016/S0006-3495(03)74715-8)
 8. J. W. Baish and K. J. Rakesh, *Fractals and cancer*, *Cancer Research* **60** (2000) 3683.
 9. A. Brú, *et al.*, Super-rough dynamics on tumor growth, *Phys. Rev. Lett.* **81** (1998) 4008. <https://doi.org/10.1103/PhysRevLett.81.4008>
 10. H. Kitano, Cancer as a robust system: implications for anti-cancer therapy, *Nature* **4** (2004) 227. <https://doi.org/10.1038/nrc1300>
 11. J.A. Llanos-Pérez *et al.*, Phase transitions in tumor growth: II prostate cancer cell lines. *Physica A: Statistical Mechanics and its Applications*, **426** (2015) 88. <https://doi.org/10.1016/j.physa.2015.01.038>
 12. J. A. Betancourt-Mar *et al.*, Phase transitions in tumor growth: IV Relationship between metabolic rate and fractal dimension of human tumor cells. *Physica A* **473** (2017) 344. <https://doi.org/10.1016/j.physa.2016.12.089>
 13. M. Itik, S. P. Banks, Chaos in a three-dimensional cancer model, *Int. J. Bifurcation Chaos* **20** (2010) 71. <https://doi.org/10.1142/S0218127410025417>
 14. A. El-Gohary, Chaos and optimal control of cancer self-remission and tumor system steady states, *Chaos Solitons Fractals* **37** (2008) 1305. <https://doi.org/10.1016/j.chaos.2006.10.060>
 15. J. A. Llanos-Pérez, J. A. Betancourt-Mar, G. Cocho, R. Mansilla and J. M. Nieto-Villar, Phase transitions in tumor growth: III vascular and metastasis behavior. *Physica A: Statistical Mechanics and its Applications* **462** (2016) 560. <https://doi.org/10.1016/j.physa.2016.06.086>
 16. S. Montero, R. Martin, R. Mansilla, G. Cocho, and J. M. Nieto-Villar, Parameters Estimation in Phase-Space Landscape Reconstruction of Cell Fate: A Systems Biology Approach. *In Systems Biology* (2018) (pp. 125-170). Humana Press, New York, NY.
 17. A. Guerra, *et al.* Phase transitions in tumor growth VI: Epithelial-Mesenchymal transition, *Physica A* (2018). DOI: [10.1016/j.physa.2018.01.040](https://doi.org/10.1016/j.physa.2018.01.040).
 18. R.R. Martin, S. Montero, M. Bizzarri, G. Cocho, R. Mansilla, and J. M. Nieto-Villar (2017). Phase transitions in tumor growth: V what can be expected from cancer glycolytic oscillations?. *Physica A: Statistical Mechanics and its Applications*, DOI: [10.1016/j.physa.2017.06.001](https://doi.org/10.1016/j.physa.2017.06.001)
 19. E. Izquierdo-Kulich, I. Rebelo, E. Tejera, and J. M. Nieto-Villar, Phase transition in tumor growth: I avascular development. *Physica A: Statistical Mechanics and its Applications*, **392** (2013) 6616. <https://doi.org/10.1016/j.physa.2013.08.010>
 20. T. Roose, S. Jonathan Chapman, and Philip K. Maini, Mathematical Models of Avascular Tumor Growth, *SIAM REVIEW* **49** (2007) 179. <https://doi.org/10.1137/S0036144504446291>
 21. E. Izquierdo-Kulich and J. M. Nieto-Villar, Mesoscopic model for tumor growth. *Math Biosci Eng* **4** (2007) 687. DOI: [10.3934/mbe.2007.4.687](https://doi.org/10.3934/mbe.2007.4.687)
 22. H. Enderling, N. Almog, L. Hlatky, *Systems biology of tumor dormancy*, vol **734** Springer Science and Business Media, (New York 2012).
 23. E. L. Stott, N. F. Britton, J. A. Glazier, and M. Zajac, Stochastic simulation of benign avascular tumour growth using the Potts model. *Mathematical and Computer Modelling*, **30** (1999) 183. [https://doi.org/10.1016/S0895-7177\(99\)00156-9](https://doi.org/10.1016/S0895-7177(99)00156-9)
 24. J. P. Freyer, and R. M. Sutherland, Regulation of growth saturation and development of necrosis in EMT6/Ro multicellular spheroids by the glucose and oxygen supply. *Cancer research*, **46** (1986) 3504.
 25. D. L. McElwain and G. Pettet, Cell Migration In Multicell Spheroids: Swimming Against the Tide. *Bull. Math. Biol.* **55** (1993) 655. <https://doi.org/10.1007/BF02460655>
 26. I. R. Cohen, A. Lajtha, J. D. Lambris, R. Paoletti *Systems Biology of Tumor Dormancy*. (2013).
 27. D. Murray, *Mathematical Biology: I. An Introduction*, Third Edition, Springer-Verlag New York Berlin Heidelberg, (2002).
 28. H. Kitano, Systems biology: a brief overview. *Science* **295** (2002) 1662. DOI: [10.1126/science.1069492](https://doi.org/10.1126/science.1069492)
 29. S. Dinicola, A systems biology approach to cancer: fractals, attractors, and nonlinear dynamics. *OMICS* **15** (2011) 93. <https://doi.org/10.1089/omi.2010.0091>
 30. M. Bizzarri (ed.), *Systems Biology, Methods in Molecular Biology, vol. 1702*, doi.org/10.1007/978-1-4939-7456-6_8
 31. Preziosi, L. (Ed.). *Cancer modelling and simulation*. CRC Press (2003).
 32. G. P. Karev, A. S. Novozhilov and E. V. Koonin, Mathematical modeling of tumor therapy with oncolytic viruses: effects of parametric heterogeneity on cell dynamics. *Biology Direct* **1** (2006).
 33. L. de Pillis and A. Radunskaya. A mathematical tumor model with immune resistance and drug therapy: An optimal control approach. *Journal of Theoretical Medicine*. **3** (2001) 79-100. <https://doi.org/10.1080/10273660108833067>
 34. G. Albano and V. Giorno, A stochastic model in tumor growth. *J. Theoretical Biol.* **242** (2006) 329. <https://doi.org/10.1016/j.jtbi.2006.03.001>
 35. C. Escudero, *Stochastic models for tumoral growth*. arXiv:q-bio.QM/0603009 17 Mar (2006).
 36. E. Izquierdo-Kulich and J. M. Nieto-Villar, Morphogenesis of the tumor patterns. *Math. Biosci. Eng.* **5** (2008) 299. DOI: [10.3934/mbe.2008.5.299](https://doi.org/10.3934/mbe.2008.5.299)
 37. E. Izquierdo-Kulich, D. Q. M. Amigó, C. M. Pérez-Amor, and J. M. Nieto-Villar, Morphogenesis and aggressiveness of cervix carcinoma. *Mathematical biosciences and engineering: MBE*, **8** (2011) 987.
 38. D. Wodarz and N. Komarova, *Computational Biology of Cancer*. Lecture Notes and Mathematical Modeling. (World Scientific, 2005).

39. S. H. Sabzpooshan and F. Pourhasanzade A new method for shrinking tumor based on microenvironmental factors: Introducing a stochastic agent-based model of avascular tumor growth. *Physica A* (2018) <https://doi.org/10.1016/j.physa.2018.05.131>
40. F. Pourhasanzade and S. H. Sabzpooshan, A cellular automata model of chemotherapy effects on tumour growth: targeting cancer and immune cells. *Math. Comput. Model Dyn. Syst.* **00** (2019) 1. <https://doi.org/10.1080/13873954.2019.1571515>
41. A. Ilachinski, *Cellular Automata*. A Discrete Universe. (World Scientific, 2001).
42. D. G. Mallet and L. G. De Pillis A cellular automata model of tumor-immune system interactions. *J Theor Biol* **239** (2006) 334. <https://doi.org/10.1016/j.jtbi.2005.08.002>
43. A. G. López, J. M. Seoane, and M. A. F. Sanjuán, Modelling Cancer Dynamics Using Cellular Automata, 2019, F. Berzovskaya, B. Toni (eds.), *Advanced Mathematical Methods in Biosciences and Applications, STEAM-H: Science, Technology, Engineering, Agriculture, Mathematics and Health*, (Springer Nature Switzerland AG 2019), https://doi.org/10.1007/978-3-030-15715-9_8
44. B. Ribba, T. Alarcon, K. Marron, P.K. Maini, and Z. Agur. The use of hybrid cellular automaton models for improving cancer therapy. Proceedings, Cellular Automata: 6th International Conference on Cellular Automata for Research and Industry, ACRI 2004, Amsterdam, The Netherlands, P.M.A. Sloot, B. Chopard, A.G. Hoekstra (Eds.), *Lecture Notes in Computer Science* **3305** (2004) 444. https://doi.org/10.1007/978-3-540-30479-1_46
45. T. S. Deisboeck *et al.* Multiscale cancer modeling. *Ann. Rev. Biomed. Eng.* **13** (2011) 127. <https://doi.org/10.1146/annurev-bioeng-071910-124729>
46. D. Basanta, B. Ribba, E. Watkin, B. You, and A. Deutsch, Computational analysis of the influence of the microenvironment on carcinogenesis. *Mathematical Biosciences*, **229** (2011) 22. <https://doi.org/10.1016/j.mbs.2010.10.005>
47. D. Hanahan and R.A. Weinberg. Hallmarks of cancer: *The next generation Cell*, **144** (2011) 646. <https://doi.org/10.1016/j.cell.2011.02.013>
48. Pourhasanzade F, Sabzpooshan SH, Alizadeh AM, Esmati E. An agent-based model of avascular tumor growth: Immune response tendency to prevent cancer development. *Simulation*. **93** (2017) 641. <https://doi.org/10.1177/0037549717699072>
49. Python Software Foundation, Python 3 version 3.7.3, March 25, 2019, Available from: <http://www.python.org>.
50. S. Wolfram, *Cellular automata and complexity*. (Collected papers. Addison Wesley, 1994).
51. E. Izquierdo-kulich, E. Alonso-becerra, J. M. Nieto-villar, Entropy Production Rate for Avascular Tumor Growth. *Journal of Modern Physics*, **2** (2011) 615. <https://doi:10.4236/jmp.2011.226071>
52. I.R. Cohen, A. Lajtha, J. D. Lambris, and R. Paoletti *Systems Biology of Tumor Dormancy*. 2013.
53. A. L. Barabasi, and H. E. Stanley, *Fractal Concepts in Surface Growth*. Cambridge University Press, (Cambridge 1995).
54. M. Mandelbrot, *Fractal Geometry of Nature*. Freeman, San Francisco, (1982).
55. U. Lucia, A. Ponzetto, and T. S. Deisboeck, A thermodynamic approach to the 'mitosis/apoptosis' ratio in cancer. *Physica A: Statistical Mechanics and its Applications* **436** (2015) 246-255.
56. L. Norton, Conceptual and Practical Implications of Breast Tissue Geometry: Toward a More Effective, Less Toxic Therapy, *Oncologist* **10** (2005) 370. DOI: 10.1634/theoncologist.10-6-370